

Viscous diffusion and photoevaporation of stellar disks

Isamu Matsuyama

*Department of Astronomy and Astrophysics, University of Toronto, Toronto, ON M5S 3H8,
Canada*

isamu@astro.utoronto.ca

Doug Johnstone

*National Research Council Canada, Herzberg Institute of Astrophysics, 5071 West Saanich
Road, Victoria, BC V9E 2E7, Canada*

doug.johnstone@nrc.ca

and

Lee Hartmann

Harvard-Smithsonian Center for Astrophysics, 60 Garden Street, Cambridge, MA 02138

lhartmann@cfa.harvard.edu

ABSTRACT

The evolution of a stellar disk under the influence of viscous evolution, photoevaporation from the central source, and photoevaporation by external stars is studied. We take the typical parameters of TTSs and the Trapezium Cluster conditions. The photoionizing flux from the central source is assumed to arise both from the quiescent star and accretion shocks at the base of stellar magnetospheric columns, along which material from the disk accretes. The accretion flux is calculated self-consistently from the accretion mass loss rate. We find that the disk cannot be entirely removed using only viscous evolution and photoionization from the disk-star accretion shock. However, when FUV photoevaporation by external massive stars is included the disk is removed in $10^6 - 10^7$ yr; and when EUV photoevaporation by external massive stars is included the disk is removed in $10^5 - 10^6$ yr.

An intriguing feature of photoevaporation by the central star is the formation of a gap in the disk at late stages of the disk evolution. As the gap starts forming, viscous spreading and photoevaporation work in resonance. When viscous

accretion and photoevaporation by the central star and external massive stars are considered, the disk shrinks and is truncated at the gravitational radius, where it is quickly removed by the combination of viscous accretion, viscous spreading, photoevaporation from the central source, and photoevaporation by the external stars. There is no gap formation for disks nearby external massive stars because the outer annuli are quickly removed by the dominant EUV flux. On the other hand, at larger, more typical distances ($d \gg 0.03\text{pc}$) from the external stars the flux is FUV dominated. As a consequence, the disk is efficiently evaporated at two different locations; forming a gap during the last stages of the disk evolution.

Subject headings: accretion, accretion disks—planetary systems: protoplanetary disks

1. Introduction

The Hubble Space Telescope (HST) has provided clear evidence of gas disks surrounding young stars in the Orion Nebula. Narrow band images reveal circumstellar disks seen in silhouette against either the background nebular light or the protoplanetary disk’s own ionization front (Bally, O’Dell, & McCaughrean 2000). These disks have been identified as “evaporating” by Johnstone, Hollenbach, & Bally (1998). Theoretically, disks should be ubiquitous. Any breaking of the spherical symmetry of the protostellar collapse will result in in-falling material being deflected from the radial direction, and disks forming around the central stars. Spherical symmetry may be broken either when the central star core is magnetized, or when the protostellar cloud has initial angular momentum. Magnetic fields tend to produce large pseudo-disks; since the material is not solely rotationally supported (Galli & Shu 1993). Alternatively, even small initial rotational velocities in the protostellar cloud produce rotationally supported disks containing most of the angular momentum of the system (Tereby, Shu, & Cassen 1984). For most theoretical models of the collapse of rotating clouds, the majority of the cloud material falls first onto the disk. Thus, as the molecular core collapses the disk mass increases. However, it is unlikely that the disk mass, M_d , becomes larger than the superior limit, $M_{max} \sim 0.3M_\star$, where M_\star is the mass of the central star. At this superior limit the disk becomes gravitationally unstable, angular momentum is transported outward by spiral density waves, and the disk accretes material toward the central star at almost the same rate as it is receiving material from the molecular core (Larson 1984).

Planet formation is an exciting possible outcome of proto-stellar disk evolution. The coplanarity and circularity of the planetary orbits in our Solar System support this notion. Explaining the origin of the Solar System and extra-solar systems requires an understanding

not only how the disks form; furthermore, we need to understand the disk evolution. In particular, the disk removal timescale and the timescale to assemble planets determine the possibility of planet formation. Shu, Johnstone, & Hollenbach (1993) proposed photoevaporation of the Solar Nebula as the gas removal mechanism that explains the differences in envelope masses between the gas-rich giants, Jupiter and Saturn; and the gas-poor giants, Uranus and Neptune. Hollenbach, Yorke, & Johnstone (2000) generalized the discussion, describing the variety of possible disk removal mechanisms. The dominant disk removal mechanism at the inner parts of the disk is viscous accretion onto the central star. However, this process is incapable of removing the entire disk in a finite time because the accretion rate decreases as the viscous disk spreads, and the disk lifetime becomes infinite. Other possible disk removal mechanisms are planet formation, stellar encounters, stellar winds or disk winds, and photoevaporation by ultraviolet photons. Hollenbach, Yorke, & Johnstone (2000) concluded that planet formation is a minor disk removal mechanism, and that the dominant mechanisms for a wide range of disk sizes are viscous accretion and photoevaporation, operating in concert within the disk.

Recently, Clarke, Gendrin, & Sotomayor (2001) have studied the observational consequences of the evolution of disks through a combination of photoevaporation and viscous disk evolution. Their study focused on photoevaporation due to ultraviolet photons produced in the disk-star accretion shock under the assumption that the accretion luminosity was constant during accretion and switched off when the inner disk was cleared. Using this model Clarke, Gendrin, & Sotomayor (2001) were able to reproduce the observed millimeter fluxes of stars with disks as a function of the observed accretion rate. In this complimentary study, we focus on the physical properties of the disk under a variety of photoevaporation and viscous scenarios in order to understand the internal disk evolution. We use a time dependent α -disk model (Shakura & Sunyaev 1973) with the parameters of Hartmann et al. (1998) that are consistent with observed mass accretion rates in T Tauri stars (TTSs). Photoevaporation by external stars is studied using the model and parameterization of Johnstone, Hollenbach, & Bally (1998), in their study of the Orion Nebula. Photoevaporation by the central star is modelled with solutions originally found for high mass stars (Hollenbach et al. 1994) and normalized to TTSs (Shu, Johnstone, & Hollenbach 1993); however, in order to study disk evolution, approximations for the time dependence of evaporation are included in the model by estimating the continual change in the accretion shock emission of ultraviolet photons as the accretion rate subsides. In agreement with Hollenbach, Yorke, & Johnstone (2000) and Clarke, Gendrin, & Sotomayor (2001), we show that it is possible to remove the entire disk in a finite time. However, we show that the rapid removal of the inner disk, described by Clarke, Gendrin, & Sotomayor (2001) is not self-consistent. We further show that gaps in the disk are a natural outcome of the combination of viscous accretion and photoevaporation

by the central star.

2. Disk Model

2.1. The thin viscous disk

With viscosity present in the disk, the energy of the shear motions between annuli is dissipated as heat, and angular momentum is transported from annuli with smaller specific angular momenta to annuli with larger specific angular momenta. If the total angular momentum in the disk is conserved a minimum energy state is approached as the inner material moves closer to the central star and the outer material spreads outward, with the outward transport of specific angular momentum (Pringle 1981). Considering angular momentum and mass conservation of an annulus of material at a radius, R , in a geometrically thin disk with viscosity, ν , the surface density evolution is described by

$$\frac{\partial \Sigma}{\partial t} = \frac{3}{R} \frac{\partial}{\partial R} \left[R^{1/2} \frac{\partial}{\partial R} (\nu \Sigma R^{1/2}) \right], \quad (1)$$

where Σ is the surface density and t is the time. In this formulation it is assumed that most of the mass is in the central star; therefore, the self gravity of the disk is ignored. The explicit evolution of the disk depends on a detailed description of the viscosity, which is weakly constrained by present observations. However, a standard approach is to assume that the viscosity is a function of the sound speed in the disk and the disk thickens. For this case, we can isolate all our uncertainty about the viscous mechanism in a dimensionless parameter, $\alpha \leq 1$, with the standard α -prescription of Shakura & Sunyaev (1973). We write

$$\nu = \alpha c_s H, \quad (2)$$

where c_s is the sound speed at the disk mid plane and H is the thickness of the disk. With this prescription the viscosity takes the form

$$\nu(R) = \alpha \frac{k}{m_p} \left(\frac{1}{GM_\star} \right)^{1/2} R^{3/2} T_d(R), \quad (3)$$

where $m_p \sim 2.3m_H$ is the mean particle mass, M_\star is the central star mass, and T_d is the disk temperature at the mid plane.

The potential energy of accreting gas is converted to thermal energy and released as radiation by viscous processes. One half of this accretion luminosity is released at the disk

surface and the other half is released at the accretion shock (see Pringle 1981). Assuming thermodynamic equilibrium, the local energy balance at each radius is described by

$$\frac{3}{8\pi} \frac{GM_*\dot{M}}{R^3} \left[1 - \left(\frac{R_*}{R} \right)^{1/2} \right] = \sigma T_s^4, \quad (4)$$

where σ is Stefan-Boltzmann constant and T_s is the disk surface temperature. For simplicity we ignore the vertical temperature gradient and assume $T_d = T_s$. Equation 4 implies a temperature distribution $T_s \propto R^{-3/4}$ for a constant accretion rate at each radius. However, the temperature distribution in the outer disk required to explain observations is much shallower, approximately $T_s \propto R^{-1/2}$ (Kenyon & Hartmann 1987). The reason for this behavior is that the optically-thick disk photosphere is curved away from the disk midplane, or flared, allowing radiation from the central star to dominate the outer disk heating (Kenyon & Hartmann 1987). Flared disk models have been shown to account for the observed disk emission satisfactorily (Chiang & Goldreich 1997; D’Alessio et al. 1998, 1999), and the dominance of stellar irradiation heating over viscous dissipation is demonstrated by the detection of silicate emission features, which arise from the temperature inversion due to external heating (Calvet et al. 1992; Chiang & Goldreich 1997).

For the observed disk temperature distribution, $T_d \propto R^{-1/2}$, the viscosity takes the simple form, $\nu(R) \propto R$, and the surface density evolution (equation 1) has analytic similarity solutions (Lynden-Bell & Pringle 1974). When only viscous accretion is considered (i.e. in the absence of photoevaporation), numerical solutions can be compared to the similarity solutions. Similarity solutions present an excellent starting condition for studying the interaction of disk evaporation and viscous evolution for various reasons. First, in the absence of photoevaporation any initial surface density distribution will diffuse to the similarity solution in the viscous diffusion timescale, $t_s = R^2/3\nu$ (see Pringle 1981), which is much shorter than the disk removal timescale. Second, we are interested in the disk evolution well after the initial disk formation during which time viscous diffusion should have produced a disk profile reasonably close to the similarity solution. Third, the formation of structure in the disk surface density due to photoevaporation occurs at late stages of the disk evolution, at timescales much longer than the viscous diffusion timescale.

We assume the observed typical parameters of TTSs. The central star has effective temperature $\sim 4000\text{K}$, luminosity $\sim 1L_\odot$, mass $\sim 0.5M_\odot$ (Johns-Krull, Valenti, & Linsky 2000). We adopt the observed disk temperature distribution (D’Alessio et al. 1998), $T_d = (10\text{K})(R/100\text{AU})^{-1/2}$. These parameters are consistent with accretion rate observations of TTSs (Hartmann et al. 1998). The initial surface density distribution is

$$\Sigma = \frac{M_d(0)}{2\pi R_0^2} \frac{1}{(R/R_0)\tau^{3/2}} e^{-(R/R_0)\tau} \quad (5)$$

where $M_d(0)$ is the initial disk mass, $R_0 = 10\text{AU}$ is a radial distance scale, and $\tau \equiv t/t_s(R_0)$ is a dimensionless time variable normalized to the viscous diffusion timescale: $t_s(R_0) = R_0^2/3\nu(R_0)$. The physical meaning of R_0 is that a fraction $1 - e^{-q}$ of the initial disk mass resides inside qR_0 . For example, $\sim 60\%$ of the mass resides inside R_0 and $\sim 90\%$ of the mass resides inside $2R_0$. Hartmann et al. (1998) estimate $\alpha \sim 10^{-2}$ from the observed disk sizes, and they show that the observed variation in mass accretion rates can be accounted for by initial disk masses between 0.01 and $0.2M_\odot$.

We solve equation 1 numerically using a backward time finite differencing scheme (Press et al. 1992). The advantage of this scheme is that it is stable for any combination of time step δt and radial distance step δR , provided the boundary conditions are well determined. It is necessary to solve a set of simultaneous linear equations at each time step given an initial density distribution and two boundary conditions. The inner boundary is $R_{min} = 10^{-2}\text{AU}$ and the outer boundary, R_{max} , is chosen such that the outer disk edge never reaches R_{max} . The boundary conditions are chosen such that the total mass and the total angular momentum in the disk are conserved. In other words, there is no input of mass or external torques at the inner or external boundaries. We define the disk edge, R_d , such that the mass between R_d and R_{max} is less than a fraction 10^{-6} of the disk mass. This assures that the contribution to the disk mass from all the annuli with $R > R_d$ is negligible.

2.2. The star disk accretion shock

The hot continuum emission or “blue veiling” present in TTs, originally explained as being due to boundary layer emission (Lynden-Bell & Pringle 1974; Bertout, Basri, & Bouvier 1988), is now thought to arise from accretion shocks at the base of stellar magnetospheric columns, along which material from the disk accretes (Königl 1991; Hartmann, Hewett, & Calvet 1994; see Hartmann 1998 and references therein). Here we assume that half of the accretion luminosity is radiated as hot continuum to write

$$L_{as} = \frac{GM_\star \dot{M}_d}{2R_\star}, \quad (6)$$

where L_{as} is the accretion shock luminosity. Magnetospheric accretion models generally assume $\sim 80\%$ of the accretion energy comes out in veiling continuum, but this difference is small in comparison with the uncertainty in the characteristic temperature.

The veiling continua of accreting T Tauri stars is not that of a simple blackbody. Nevertheless, it appears that the FUV continuum can be roughly approximated as having a characteristic temperature $\sim 10,000\text{K}$ (Johns-Krull, Valenti, & Linsky 2000; Gullbring et

al. 2000). There is no constraint on the EUV fluxes due to interstellar absorption. In the following we assume that the FUV and EUV fluxes can be characterized as blackbody emission at $T = 1.5 \times 10^4\text{K}$, which may somewhat overestimate the amount of short-wavelength radiation.

2.3. The hot ionized disk atmosphere

The EUV ($h\nu > 13.6\text{eV}$) photons from the central star, the accretion shock, or the external stars are capable of ionizing hydrogen and evaporating material from the disk surface. This mechanism affects the disk surface layer and forms an ionized atmosphere above the thin viscous disk. Hollenbach et al. (1994) describe analytical solutions for this atmosphere assuming a typical H II region temperature, T_{II} , of 10^4K . The equilibrium temperature arises from balance between heating, due primarily to incident ionizing photons; and cooling, due primarily to forbidden line radiation. Using Euler's equation and assuming hydrostatic equilibrium in the z -direction, we can write the number density of electrons for an isothermal atmosphere as

$$n(R, z) = n_0(R, z = 0)e^{-z^2/2H^2}, \quad (7)$$

where $n_0(R)$ is the number density at the disk base $z = 0$ and

$$H = c_{sII} \left(\frac{R}{GM_\star} \right)^{1/2}, \quad (8)$$

is the scale height. In the last equation

$$c_{sII} = \left(\frac{kT_{II}}{m_{II}} \right)^{1/2} \quad (9)$$

is the isothermal sound speed of the gas at temperature, T_{II} , and mean particle mass, $m_{II} = 1.13 \times 10^{-24}$ g. The scale height grows with increasing R until it becomes equal to R at the gravitational radius,

$$R_{gII} \equiv \frac{GM_\star}{c_{sII}^2}. \quad (10)$$

The relevance of this radius is not only geometrical, but also dynamical. The sum of the kinetic energy and the thermal energy per unit mass at the gravitational radius is

$$\frac{1}{2}\Omega^2 R_{gII}^2 + \frac{3kT_{II}}{2m_{II}} = \frac{2GM_\star}{R_{gII}}, \quad (11)$$

where $\Omega = (GM_\star/R_{gII}^3)^{1/2}$ is the Keplerian angular velocity. Gas material has twice the negative energy of the gravitational potential energy, that is, it has more than enough energy to escape to infinity as a disk wind at R_{gII} . Shu, Johnstone, & Hollenbach (1993) show that the gravitational radius for the Solar nebula is at the orbital distance of Saturn, giving a possible explanation for the sharp differences in envelope masses between the gas-rich giants, Jupiter and Saturn, and the gas-poor giants, Uranus and Neptune. Since the gas material at R_{gII} already has more than the minimum energy to escape, some mass loss occurs even inside R_g , and gas particles become gravitationally bound to the central star at a location between the central star radius, R_\star , and the gravitational radius. We characterize this by assuming that the effective gravitational radius is βR_{gII} , where $R_\star/R_{gII} < \beta < 1$. An additional factor that makes β smaller is the fact that material can also be removed inside R_{gII} due to the pressure gradients in the flow. We use an effective gravitational radius characterized by $\beta = 0.5$, i.e. we assume that the gas material in the ionized atmosphere is gravitationally bound to the central star for $R < 0.5R_{gII}$.

2.4. The warm neutral disk atmosphere

The FUV ($6 < h\nu < 13.6\text{eV}$) photons from the central star, the accretion shock, or external stars; capable of dissociating H_2 and CO ; also affect the disk structure. The FUV photons penetrate the ionized region and create a neutral hydrogen layer with temperature, $T_I \sim 10^3\text{K}$. Following the same arguments for the ionized atmosphere, we can define a gravitational radius for the neutral layer as

$$R_{gI} \equiv \frac{GM_\star}{c_{sI}^2}. \quad (12)$$

The isothermal sound speed at the neutral layer is given by

$$c_{sI} = \left(\frac{kT_I}{m_I} \right)^{1/2}, \quad (13)$$

where $m_I = 1.35m_H$ is the mean particle mass per hydrogen atom.

3. Disk evolution and photoevaporation

3.1. EUV photoevaporation from the central source

Hollenbach et al. (1994) found analytic solutions for the photoevaporation mass loss rate by EUV photons from the central star. These photons are attenuated by recombined

hydrogen atoms and scattering from dust in the ionized atmosphere; providing a source of diffuse EUV photons. The ionized atmosphere absorbs a significant fraction of the direct incident flux, and the diffuse field dominates the flux onto the disk. Disk material is gravitationally bound inside the gravitational radius, R_{gII} , and it flows out the disk base at the sound speed, c_{sII} , outside the gravitational radius. Given the number density of ionized hydrogen at the disk base, $n_0(R)$, we can calculate the evaporation rate:

$$\dot{\Sigma}(R) = \begin{cases} 2m_{II}n_0(R)a_{II}, & \text{if } R > \beta R_{gII}; \\ 0, & \text{otherwise;} \end{cases} \quad (14)$$

where the factor of two accounts for photoevaporation from both sides of the disk. A self-regulating mechanism is established at the disk base and it is possible to find the number density in this region. If the number density at the disk base were lower than the equilibrium value, the diffuse EUV photons would penetrate deeper into the disk, producing more ionizations, and the number of ionized hydrogen would increase. On the other hand, if the number density were higher than the equilibrium value, the recombinations and the scattering from dust in the ionized atmosphere would prevent the diffuse EUV photons from reaching the disk base, and the number of ionizations would decrease.

Assuming ionization equilibrium Hollenbach et al. (1994) found the number density at the disk base for the “weak” and “strong” stellar wind cases. In the weak stellar wind case, the stellar wind ram pressure is smaller than the thermal pressure for $R < \beta R_{gII}$ and the atmosphere is static. Gas material is evaporated at the rate given by equation 14 outside the gravitational radius. The dominant flux of EUV photons producing the flow is from the diffuse field that shines vertically downward onto the disk at the gravitational radius; therefore, most of the gas is evaporated from this region. In the strong stellar wind case, the stellar wind ram pressure is higher than the thermal pressure even outside βR_{gII} . Although disk material evaporates in the vicinity of βR_{gII} , the dominant flow occurs where the stellar wind ram pressure equals the thermal pressure, at a characteristic radius, $R_w > \beta R_{gII}$. Due to large uncertainties in both the wind mass loss rate, the effects of collimation in the wind, and the ionization flux from the central star, it is not clear whether or not the strong wind condition is met for low mass stars (Hollenbach, Yorke, & Johnstone 2000). Here, we only consider the weak stellar wind case. The number density at the disk base for the weak stellar wind case is

$$n_0(R) = \begin{cases} 5.7 \times 10^5 \phi_{40}^{1/2} R_{13}^{-3/2} \text{ cm}^{-3}, & \text{if } R \leq \beta R_{gII}; \\ n_0(\beta R_{gII}) (R/\beta R_{gII})^{-5/2}, & \text{otherwise;} \end{cases} \quad (15)$$

where ϕ_{40} is the ionizing photon luminosity in units of 10^{40}s^{-1} and R_{13} is the radius in units of 10^{13}cm .

Clarke, Gendrin, & Sotomayor (2001) used essentially the same model for the photoevaporation component of disk dispersal; however, they assumed that the ionizing flux was constant during the disk evolution. In contrast, we explicitly model the ultraviolet photons produced in the accretion layer as a function of time. The total ionizing flux is $\phi = \phi_\star + \phi_{as}$, where ϕ_\star is the ionizing flux from the stellar photosphere and ϕ_{as} is the ionizing flux from the accretion shock. We assume the parameters of typical TTSs under the assumption that only the quiescent star produces ultraviolet photons. In fact, these stars are chromospherically active (Feigelson & Montmerle 1999), providing an additional source of ionizing photons. However, both the time dependence of the chromospheric activity and the rate of ionizing photon production are poorly constrained at present and thus we take the limiting case of an insignificant chromosphere. The luminosity is $L_\star = 1L_\odot$, the surface temperature is $T_\star = 4000\text{K}$, and the accretion shock temperature is $T_{as} = 1.5 \times 10^4\text{K}$ (Johns-Krull, Valenti, & Linsky 2000; Kenyon et al. 1989). We calculate the accretion luminosity using equation 6, and the fraction of ionizing photons from this luminosity with the accretion shock temperature. For illustration, figure 1a plots the corresponding ionizing flux for typical accretion rates during the disk evolution. The constant ionizing flux ($\phi = 10^{41}\text{s}^{-1}$) assumed by Clarke, Gendrin, & Sotomayor (2001) is only produced for high accretion rates ($\dot{M} \sim 10^{-8}\dot{M}_\odot\text{yr}^{-1}$) at early stages of the disk evolution. We plot in figure 1b the time dependence of the ionizing flux for several possible disk scenarios that cover the parameter space of observations. It is clear that the ionizing flux is not constant, it decreases with the accretion rate as the disk loses its mass. Even for high viscosities, $\alpha \sim 10^{-2}$, and initially massive disks, $M_d(0) \sim 10^{-1}M_\odot$, corresponding to high initial accretion rates, the ionizing flux decreases to values well below $\sim 10^{41}\text{s}^{-1}$. Thus, it is essential to compute the ionizing flux self-consistently from the accretion luminosity when considering photoevaporation from the inner disk.

Combining photoevaporation with viscous accretion is done numerically. At each time step, photoevaporation induced mass loss and viscous accretion induced disk evolution are solved, with the time step chosen such that the mass removed due to each mechanism is negligible compared to the instantaneous disk mass. The mass removal rate by photoevaporation is determined by equation 14 and the surface density, since it is only possible to photoevaporate material at locations where $\Sigma > 0$.

Figure 2 shows snapshots of the surface density distribution for two representative cases: a model with high viscosity ($\alpha = 10^{-2}$) and a massive initial disk ($M_d(0) = 10^{-1}M_\odot$), and a model with low viscosity ($\alpha = 10^{-3}$) and a small initial disk ($M_d(0) = 10^{-2}M_\odot$). In both cases a gap structure forms during the later stages of the disk evolution. Disk material is accreted toward the central star and photoevaporation from the central source removes material outside the gravitational radius. Figure 3 shows the remaining disk mass, the disk mass

accreted toward the central star, and the disk mass removed by photoevaporation. Most of the initial disk mass is accreted toward the central star in both cases. Photoevaporation removes all the material in the vicinity of the gravitational radius when the surface density at this radius is low ($\sim 10^{-1}\text{g cm}^{-2}$), and divides the disk into an inner and an outer annulus. The subsequent evolution is dominated by two counteracting effects; viscous diffusion attempts to spread both annuli and remove the gap structure while photoevaporation removes material predominantly at the gravitational radius and reopens the gap. The outcome of the combination of the two mechanisms is an efficient mass removal from the disk. Disk material at the outer edge of the inner annulus is viscously spread beyond the gravitational radius, where it is removed by photoevaporation. Clarke, Gendrin, & Sotomayor (2001) showed that it is possible to quickly remove the inner disk; however, we show that the inner disk is removed at the same rate as the outer disk. This difference arises because Clarke, Gendrin, & Sotomayor (2001) assume a constant ionizing flux while we calculate the ionizing flux from the accretion luminosity. In our model, the ionizing flux from the accretion shock decreases (see figure 1b) as the accretion rate decreases (see figure 4) until it reaches the constant value ($1.29 \times 10^{31}\text{s}^{-1}$) corresponding to the quiescent stellar photosphere. Therefore, removing the inner disk and maintaining a high ionizing flux ($\sim 10^{41}\text{s}^{-1}$) is not self-consistent. It is not possible to remove the inner disk faster than the outer disk even for high accretion shock temperatures ($T_{as} \sim 3 \times 10^4\text{K}$) that correspond to stronger ionizing fluxes. The strong dominance of viscous diffusion over photoevaporation (see figures 3 and 4) produce unrealistically long disk lifetimes ($\sim 10^{12} - 10^{13}\text{yr}$; see figure 3) unless the stellar ionizing flux is extremely enhanced through an active chromosphere (Figure 1b can be used to estimate the time at which this model would break down if the chromospheric activity produced a significant ionizing flux ϕ_{ch} . For example, if $\phi_{ch} = 10^{35}\text{s}^{-1}$ for more than $\sim 10^9\text{yr}$ then the calculated models would begin to diverge from reality.) It is not possible to quickly remove the inner annulus due to the vanishing ionizing flux. However, as the outer annulus spreads to distances far from the gravitational radius where photoevaporation becomes inefficient, other removal mechanisms such as stellar encounters become important and will limit the disk lifetime.

3.2. EUV photoevaporation by external stars

Stellar disks are also dispersed by external stars and this is a likely situation for the disks surrounded by ionization fronts in the Trapezium Cluster (Bally, O’Dell, & McCaughrean 2000). Johnstone, Hollenbach, & Bally (1998) found models for EUV dominated external photoevaporation based on observations of the proplyds in the Orion Nebula. In this scenario the disk is heated by UV photons from the nearby O stars. Since the inner annuli have a

small surface area compared to the outer annuli, their contribution to the process is very small. Most of the material is removed at the disk edge, R_d , and photoevaporation from the disk can be approximated by photoevaporation from a sphere with radius R_d . The EUV photons control the flux close to the central star; heating the gas to $T_{\text{H II}} \sim 10^4\text{K}$ and creating an ionization front. Following Johnstone, Hollenbach, & Bally (1998), the mass loss rate for EUV photoevaporation can be approximated by

$$\dot{M}_d^{EUV} = \begin{cases} 7 \times 10^{-12} \text{ M}_\odot \text{ yr}^{-1} \left(\frac{\Phi_i}{10^{49}\text{S}^{-1}}\right)^{1/2} \left(\frac{1\text{pc}}{d}\right) \left(\frac{R_d}{1 \text{ AU}}\right)^{3/2}, & \text{if } R_d > \beta R_{gII}; \\ 0, & \text{otherwise;} \end{cases} \quad (16)$$

where ϕ_i is the ionization rate of the external star and d is the distance to the external star. Most of the mass is evaporated from the outer disk annuli because they have the largest surface area. We assume the Trapezium Cluster conditions, where most of the flux, $\phi_i \sim 10^{49}\text{s}^{-1}$ is from θ^1 Ori C. The EUV photons dominate the flux for the proplyds orbiting at a distance $d \lesssim 0.03\text{pc}$ from the external star (Johnstone, Hollenbach, & Bally 1998; Störzer & Hollenbach 1999), and we assume $d = 0.02\text{pc}$ in the following models. The surface density evaporation rate is the mass loss rate divided by the effective area of the disk:

$$\dot{\Sigma}^{EUV}(R) = \begin{cases} \frac{\dot{M}_d^{EUV}}{\pi(R_d^2 - \beta^2 R_{gII}^2)}, & \text{if } R > \beta R_{gII}; \\ 0, & \text{otherwise.} \end{cases} \quad (17)$$

The disk is removed due to accretion toward the central star, photoevaporation from the central source, and EUV photoevaporation by the external stars. The disk evolution is strongly affected by the external radiation field. Photoevaporation by the external star dominates the ionizing flux at large radii where material is efficiently evaporated. Hence, photoevaporation by the central star is a minor disk removal mechanism. We show the results for two models with the same parameters as before (see section 3.1). Figure 5 shows snapshots of the surface density distribution. Viscous diffusion spreads the disk in both directions and photoevaporation from the external star removes the outer parts; as a result, the disk size remains constant (at the gravitational radius) until just before the disk is completely removed. The disk truncation is in good agreement with the two dimensional simulations of Richling & Yorke (2000). However, their simulation stops at $t \sim 10^4\text{yr}$, before the disk is completely removed. There is no formation of gap structures due to the strong dominance of EUV photoevaporation from the external stars over photoevaporation from the central source. The disk is quickly removed as viscous accretion, photoevaporation by the central star, and EUV photoevaporation by the external star work in resonance. The strong dominance of photoevaporation by the external star is also illustrated in the total

mass removed by photoevaporation (see figure 6) and the mass removal rate (see figure 7). Photoevaporation by the external stars removes most of the disk mass and changes dramatically the disk evolution, in particular, it is possible to completely remove the disk in $\sim 10^6$ yr.

3.3. FUV photoevaporation by external stars

While the EUV photons create an ionization front and heat the gas to the temperature, $T_{\text{H II}} \sim 10^4\text{K}$, the FUV photons penetrate this ionized region and heat a neutral hydrogen layer to the temperature, $T_{\text{H I}} \sim 10^3\text{K}$. At large distances from the external star the FUV photons dominate and the neutral layer launches a supersonic flow. Johnstone, Hollenbach, & Bally (1998) also found models for FUV dominated external photoevaporation based on observations of the proplyds in the Orion Nebula. The mass loss rate by photoevaporation can be approximated by

$$\dot{M}_d^{FUV} = \begin{cases} 2 \times 10^{-9} \text{ M}_\odot \text{ yr}^{-1} \left(\frac{N_D}{5 \times 10^{21} \text{ cm}^{-2}} \right) \left(\frac{R_d}{1 \text{ AU}} \right), & \text{if } R_d > R_{gI}; \\ 0, & \text{otherwise;} \end{cases} \quad (18)$$

where N_D is the column density from the ionization front to the disk surface, and R_{gI} is the gravitational radius for the neutral layer. In the following models it is assumed that $N_D \sim 5 \times 10^{21} \text{ cm}^{-2}$ based on the numerical results of Störzer & Hollenbach (1998). The surface density photoevaporation rate for the FUV dominated flow is the mass loss rate divided by the effective area of the disk:

$$\dot{\Sigma}^{FUV}(R) = \begin{cases} \frac{\dot{M}_d^{FUV}}{\pi(R_d^2 - \beta^2 R_{gI}^2)}, & \text{if } R > \beta R_{gI}; \\ 0, & \text{otherwise.} \end{cases} \quad (19)$$

The disk mass is removed due to viscous accretion toward the central star, photoevaporation from the central source, and FUV photoevaporation by the external stars. For the Trapezium Cluster, the FUV photons dominate the flux for the proplyds orbiting at a distance $d \gg 0.03\text{pc}$ from the external stars (Johnstone, Hollenbach, & Bally 1998; Störzer & Hollenbach 1999).

We show the results for the two representative models with the same parameters as before. Figure 8 shows snapshots of the surface density evolution. The outer disk ($R > R_{gI}$) is removed by FUV photoevaporation from the external stars. As a result, the disk edge is reduced to the FUV gravitational radius. The disk size remains roughly constant at this radius until the disk is completely removed. At the final stages of the disk evolution

($t \sim t_{gap}$), when the surface density is very low ($\Sigma \sim 10^{-5} \text{g cm}^{-2}$), a gap structure is created by photoevaporation from the central source. The gap formation is possible because photoevaporation from the central source and photoevaporation by the external stars are dominant at different locations (R_{gII} and R_{gI}). Both annuli are removed as viscous accretion, viscous spreading, and photoevaporation work in resonance (see figures 10 and 11). The outer annulus is removed by the combination of viscous spreading, photoevaporation from the central source, and photoevaporation by the external stars. On the other hand, the inner annulus is removed by the combination of viscous accretion toward the central star, viscous spreading, and photoevaporation from the central source. The efficient inner disk removal is self-consistent since we have calculated the ionizing flux from the accretion luminosity and the quiescent stellar photosphere. As the inner disk is removed, the contribution from the accretion luminosity becomes negligible; as a result, the ionizing flux reaches the value corresponding to the quiescent stellar photosphere, $\phi_{\star} = 1.29 \times 10^{31} \text{s}^{-1}$ (figure 9). Again, the active chromosphere of these low-mass stars has not been included; however, in this situation the lack of chromospheric ionizing flux is much less important as the timescale for disk evaporation has been set by the disk truncation due to the external source.

4. Discussion and summary

We have studied the possibility of disk removal by the combination of viscous diffusion and photoevaporation, assuming that the ultraviolet photons responsible for evaporation arises either from the quiescent stellar photosphere, the accretion shock, or external O stars. It is not possible to remove the entire disk when the only disk removal mechanism is viscous accretion: the disk spreads indefinitely in order to conserve total angular momentum while material is accreted onto the central star. Mass loss due to photoevaporation removes material along with its specific angular momentum; thus, it is possible to accrete material toward the central star and reduce the amount of disk spreading. The combination of the two mechanisms can result in finite disk lifetimes.

The distinctive features of photoevaporation by the ionizing flux from the central source are the formation of a gap around the EUV gravitational radius at late stages of the disk evolution and the lack of a finite time for the complete dispersal of the disk. The gap forms for the observed range of accretion shock temperatures ($1 - 3 \times 10^4 \text{K}$) and the disk becomes divided into an inner and an outer annulus. The inner annulus continues to be removed by the combination of viscous accretion, viscous spreading of material beyond the EUV gravitational radius, and photoevaporation at this radius. The outer annulus is removed as viscous spreading of material toward the gravitational radius and photoevaporation work in

resonance. Clarke, Gendrin, & Sotomayor (2001) considered models with photoevaporation by a constant central ionizing flux combined with viscous evolution, and showed that the timescales to remove the inner and the outer annuli are not the same. We conclude that this result is due to their assumption of a constant ionizing flux. In contrast, we calculate the ionizing flux from the accretion luminosity self-consistently. We find that both the inner and outer disks survive to much longer times, and that the inner disk is *not* removed first. It is not possible to quickly remove the inner annuli and maintain a high ionizing flux at the same time because the accretion rate decreases. The formal disk lifetime is found to be in the range $10^{12} - 10^{13}$ yr for $10^{-3} < \alpha < 10^{-2}$ and $10^{-2} < M_d(0) < 10^{-1}$, much longer than the star lifetime. Introducing a stellar chromosphere will produce models intermediate between those presented here and those of Clarke, Gendrin, & Sotomayor (2001).

Stellar disk material can also be evaporated by external stars. This is a likely situation for the disks surrounded by ionization fronts in the Trapezium Cluster (Johnstone, Hollenbach, & Bally 1998; Störzer & Hollenbach 1999; Bally, O’Dell, & McCaughrean 2000). The EUV photons dominate the flux for the proplyds orbiting at a distance $d \lesssim 0.03$ pc, and the FUV photons dominate for the proplyds at more typical ($d \gg 0.03$ pc) distances from the massive external stars.

We consider photoevaporation due to both the central source and external stars. There is no gap formation for disks nearby external hot stars since their ionizing flux removes all the disk material outside the EUV gravitational radius. The disk is quickly removed by viscous accretion, viscous spreading, and photoevaporation outside the gravitational radius. The disk lifetime is in the range $10^5 - 10^6$ yr for the same parameters as before, where the shorter lifetimes correspond to shorter viscous evolution timescales of high viscosities. The disk lifetimes are shorter by roughly two orders of magnitude when compared to the models with only photoevaporation from the central source. The short disk lifetimes are due to the strong influence of the external radiation field at the outer disk, where most of the disk mass initially resides.

The disk evolution is very different at larger, more typical distances ($d \gg 0.03$ pc) from the external stars due to the different locations where photoevaporation is efficient. The disk material in the vicinity of the EUV gravitational radius is removed by photoevaporation from the central source. Similarly, the disk material in the neighborhood of the FUV gravitational radius is removed by external FUV photoevaporation. The effect of external photoevaporation is initially very dominant; quickly reducing disk size to the FUV gravitational radius. After this disk truncation, the disk mass is removed at two locations. At the inner edge, disk material is viscously accreted onto the central. On the other hand, viscous diffusion spreads the disk material beyond the FUV gravitational radius, and FUV photoevaporation removes

the disk material at this location. The combination of these mechanisms decreases the disk surface density. At the last stages of the disk evolution, when the surface density is very low ($\Sigma \sim 10^{-4} \text{g cm}^{-2}$), the ionizing flux from the central source opens a gap in the disk. In this case, it is possible to remove the inner annulus faster than the outer one self-consistently. The disk lifetime is in the range $10^6 - 10^7 \text{yr}$ for the same parameters as before, where the shorter disk lifetimes correspond to the shorter viscous evolution timescales of high viscosities.

Observations suggest that the timescale for all the stars in young clusters to lose their disks is $\sim 6 \times 10^6 \text{yr}$ (Haisch, Lada, & Lada 2001), in agreement with the disk lifetimes for the proplyds nearby external hot stars ($10^5 - 10^6 \text{yr}$). The disk removal timescale is an important constraint on the timescale allowed for planet formation. It is very attractive to study the possibility of planet formation in star forming regions since this process follows star and disk formation. If the influence of massive external stars in star forming regions is not demolishing for planet formation, star forming regions are natural birthplaces of extrasolar planets. Numerical simulations suggest a timescale for terrestrial planet formation in the range $10^7 - 10^8 \text{yr}$ (Beauge & Aarseth 1990; Chambers 2001), and a typical timescale for giant planet formation that range from a few million years to more than 10^7yr (Bodenheimer, Hubickyj, & Lissauer 2000; Ikoma, Nakazawa, & Emori 2000). It is thus not possible to form planets around stars in the neighborhood of massive O stars (i.e. EUV external photoevaporation) because the disk lifetime is too short ($10^5 - 10^6 \text{yr}$). On the other hand, at typical distances from the external stars ($d \gg 0.03 \text{pc}$), the disk lifetimes are long enough ($10^6 - 10^7 \text{yr}$) to allow for the formation of terrestrial and giant planets. There are no constraints on planet formation in the absence of EUV or FUV fluxes from external stars.

We would like to thank Norman Murray and Gibor Basri for helpful comments and discussions. The research of D.J. and I.M. was supported through a grant from the Natural Sciences and Engineering Council of Canada. The research of I.M. was supported by the Connaught Scholarship of the University of Toronto.

REFERENCES

- Bally, J., O'Dell, C. R., & McCaughrean, M. J. 2000, *ApJ*, 119, 2919
- Beauge, C., & Asset, S. J. 1990, *MNRAS*, 245, 30
- Bertout, C., Basri, G., & Bouvier, J. 1988, *ApJ*, 330, 350
- Bodenheimer, P., Hubickyj, O., & Lissauer, J.J. 2000, *ICARUS*, 143, 2

- Calvet, N., Magris, G.C., Patiño, A., & D'Alessio, P. 1992, *Revista Mexicana de Astronomia y Astrofisica*, 24, 27
- Chambers, J.E. 2001, *ICARUS*, 152, 205
- Chiang, E.I. & Goldreich, P. 1997, *ApJ*, 490, 368
- Clarke, C.J., Gendrin, A., & Sotomayor, M. 2001, *MNRAS*, 328, 485
- D'Alessio, P., Cantó, J., Calvet, N., & Lizano, S. 1998, *ApJ*, 500, 411
- D'Alessio, P., Calvet, N., Hartmann, L., Lizano, S., & Cantó, J. 1999, *ApJ*, 527, 893
- Feigelson, E. D. & Montmerle, T. 1999, *ARA&A*, 37, 363
- Galli D., & Shu, F. H. 1993, *ApJ*, 417, 220
- Gullbring, E., Calvet, N., Muzerolle, J., & Hartmann, L. 2000, *ApJ*, 544, 927
- Haisch, K. E., Jr., Lada, E. A., & Lada, C. 2001, *ApJ*, 553, L153
- Hartigan, P., Edwards, S., & Ghandour, L. 1995, *ApJ*, 452, 736
- Hartmann, L. 1998, *Accretion processes in star formation* (Cambridge University Press)
- Hartmann, L., Calvet, N., Gullbring, E., & D'Alessio, P. 1998, *ApJ*, 495, 385
- Hartmann, L., Hewett, R., & Calvet, N. 1994, *ApJ*, 426, 669
- Hollenbach, D.J., Johnstone, D., Lizano, S., & Shu, F. 1994, *ApJ*, 428, 654
- Hollenbach, D., Yorke, H.W., & Johnstone, D. 2000, in *Protostars and Planets IV*, ed. V. Mannings, A. P. Boss, & S. S. Russell (Tucson: Univ. Arizona Press), 401
- Ikoma, M., Nakazawa, K., & Emori, H. 2000, *ApJ*, 537, 1013
- Johns-Krull, C.M., Valenti, J.A., & Linsky J. L. 2000 *ApJ*, 539, 815
- Johnstone, D., Hollenbach, D., & Bally, J. 1998, *ApJ*, 499, 758
- Kenyon, S.J. & Hartmann, L. 1987, *ApJ*, 323, 714
- Kenyon, S.J., Hartmann, L., Imhoff C.L., & Cassatella A. 1989, *ApJ*, 344, 925
- Königl, A. 1991, *ApJ*, 370, 39
- Larson, R.B. 1984, *MNRAS*, 206, 197L

- Lynden-Bell, D. & Pringle, J.E. 1974, MNRAS, 168, 603
- Press, W., Teukolsky, S.A., Vetterling, W.T., & Flannery B.P. 1992, Numerical Recipes in C, Cambridge University Press
- Pringle, J.E. 1981, ARA&A, 19, 137
- Richling, S., & Yorke, H.W. 2000, ApJ, 539, 258
- Shakura, N.I. & Sunyaev, R.A. 1973, A&A, 24, 337
- Shu, F.H., Johnstone, & Hollenbach, D. 1993, Icarus, 106, 92
- Störzer, H., & Hollenbach, D. 1998, ApJ, 495, 853
- Störzer, H., & Hollenbach, D. 1999, ApJ, 515, 669
- Tereby, S., Shu, F. H., & Cassen, P. 1984, ApJ, 286, 551

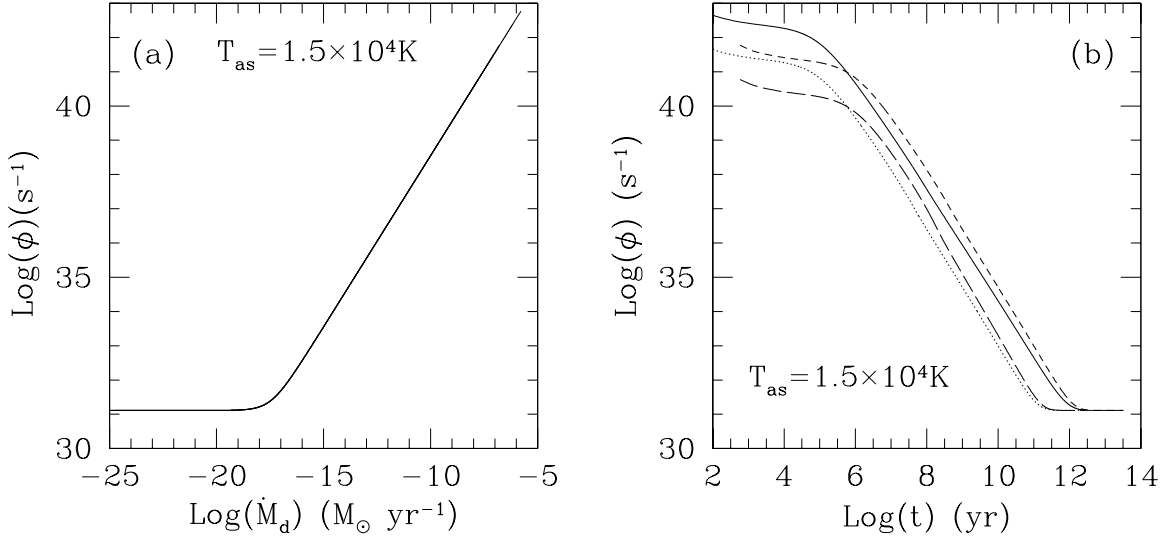


Fig. 1.— Number of ionizing photons, ϕ , as a function of accretion rate and disk lifetime for different disk parameters that cover the parameter space from observations. Solid line with parameters, $\alpha = 10^{-2}$ and $M_d(0) = 10^{-1} M_\odot$. Dotted line, $\alpha = 10^{-3}$ and $M_d(0) = 10^{-1} M_\odot$. Short-dashed line, $\alpha = 10^{-2}$ and $M_d(0) = 10^{-2} M_\odot$. Long-dashed line, $\alpha = 10^{-3}$ and $M_d(0) = 10^{-2} M_\odot$. The disk is removed by viscous accretion and photoevaporation from the central source. The ionizing flux approaches the constant value ($\phi = 1.29 \times 10^{31} \text{ s}^{-1}$) corresponding to the quiescent stellar photosphere at late stages of the disk evolution when the accretion rates are very small.

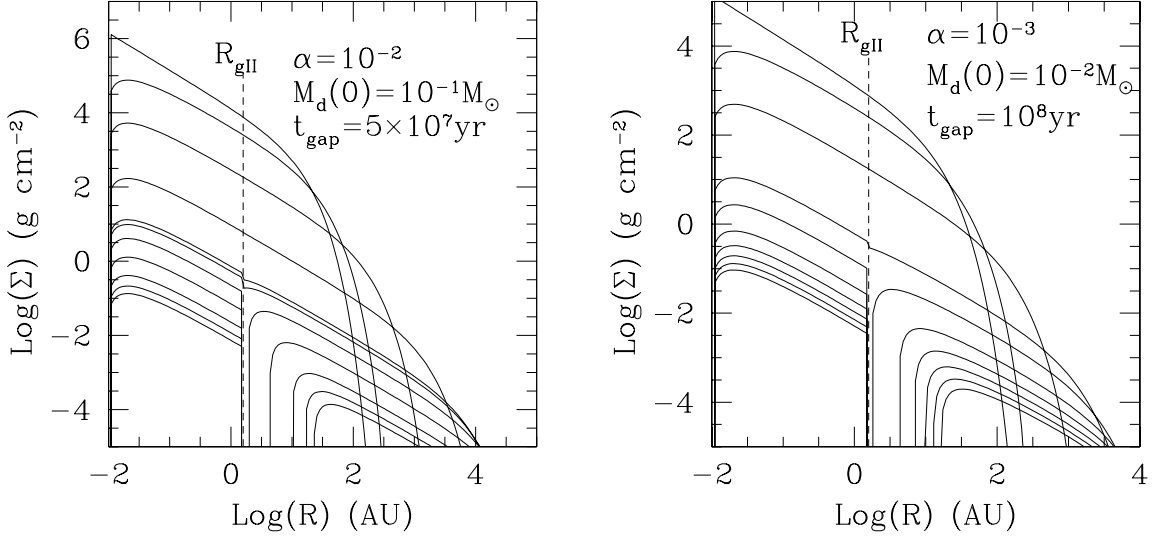


Fig. 2.— Snapshots of the surface density for two representative models under the influence of viscous diffusion and photoevaporation from the central source. The short-dashed lines indicate the location of the gravitational radius, r_{gII} ; and t_{gap} is the time when gap structures start forming. Left, model with high viscosity ($\alpha = 10^{-2}$) and massive initial disk ($M_d(0) = 10^{-1} M_\odot$). The curves represent $t = 0, 10^5, 10^6, 10^7, 5 \times 10^7, 6 \times 10^7, 10^8, 2 \times 10^8, 4 \times 10^8, 6 \times 10^8, \text{ and } 8 \times 10^8 \text{ yr}$. A gap structure starts forming at $t \sim 5 \times 10^7 \text{ yr}$, when the disk mass is $\sim 3 \times 10^{-3} M_\odot$. The disk mass corresponding to the last surface density distribution shown (at $t = 8 \times 10^8 \text{ yr}$) is $\sim 10^{-4} M_\odot$. Right, model with low viscosity ($\alpha = 10^{-3}$) and small initial disk ($M_d(0) = 10^{-2} M_\odot$). The curves represent $t = 0, 10^6, 10^7, 10^8, 2 \times 10^8, 4 \times 10^8, 6 \times 10^8, 8 \times 10^8, 10^9, \text{ and } 1.2 \times 10^9 \text{ yr}$. A similar gap structure starts forming at $t \sim 10^8 \text{ yr}$, when the disk mass is $\sim 10^{-3} M_\odot$. The disk mass corresponding to the last surface density distribution shown (at $t = 1.2 \times 10^9 \text{ yr}$) is $\sim 10^{-4} M_\odot$.

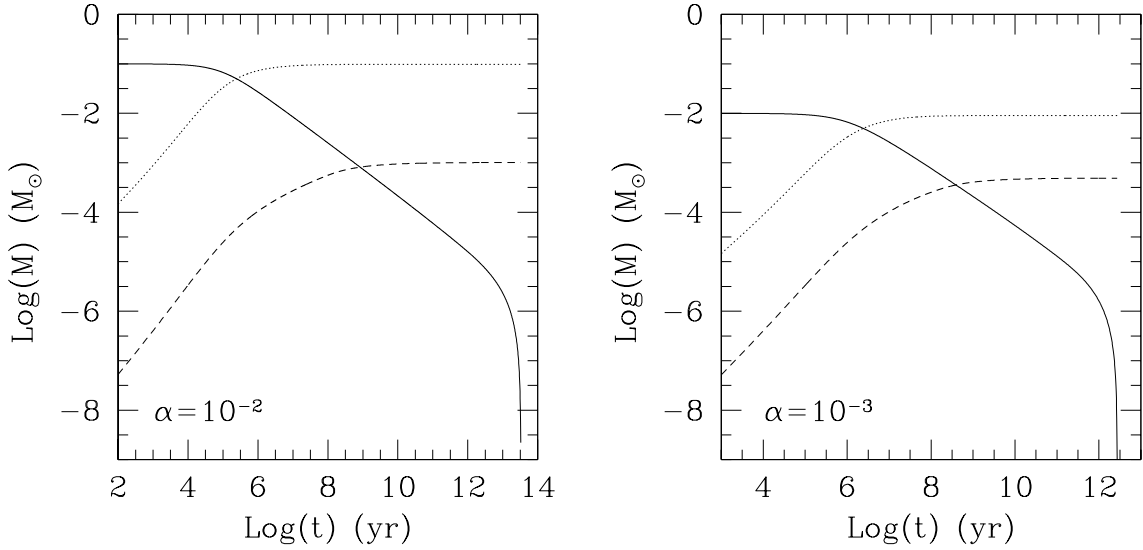


Fig. 3.— Disk mass (solid line), disk mass accreted toward the central star (dotted line), and disk mass removed by photoevaporation from the central source (short-dashed line) as a function of disk lifetime for the two representative models. The disk is removed due to viscous diffusion and photoevaporation from the central source.

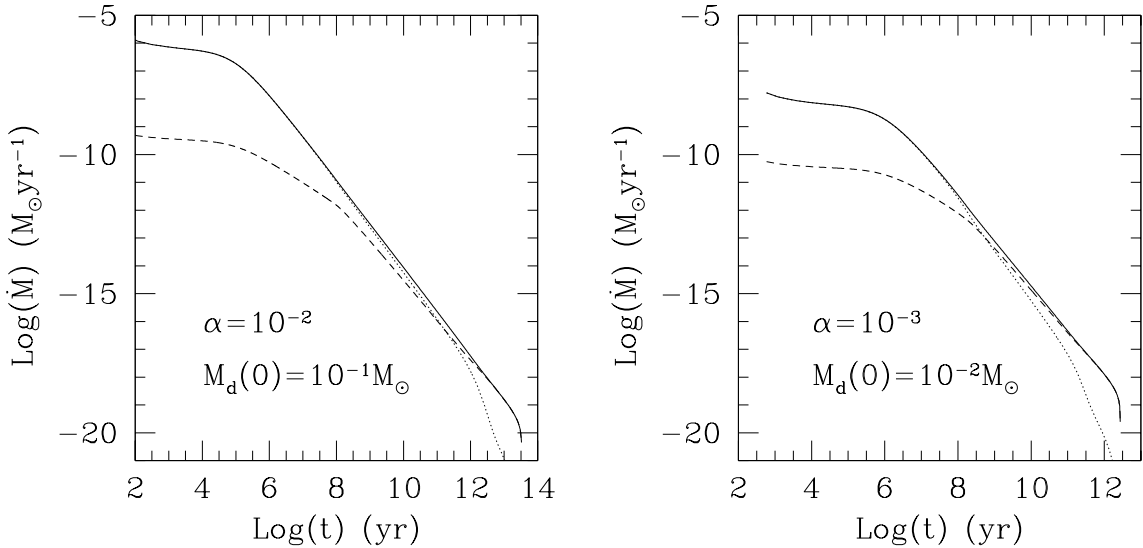


Fig. 4.— Total mass removal rate (solid line), mass removal rate due to accretion (dotted line), and mass removal rate due to photoevaporation by the central source (short-dashed line) vs. disk lifetime for the two representative models.

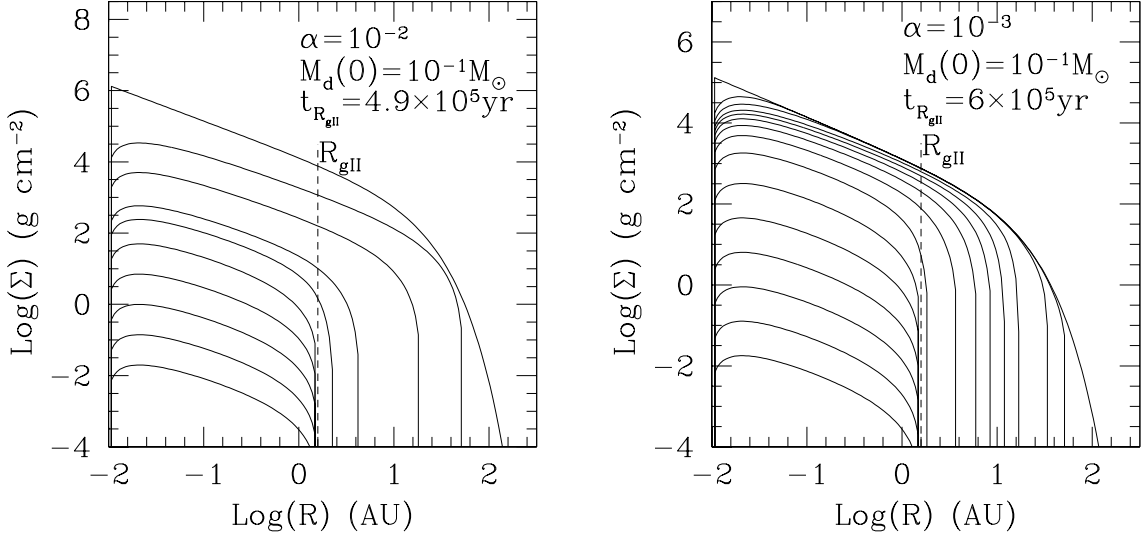


Fig. 5.— Snapshots of the surface density for two representative models considering viscous diffusion, photoevaporation from the central source, and EUV photoevaporation by external stars. The dashed lines indicate the location of the EUV gravitational radius, r_{gII} ; and t_{gap} is the time when gap structures start forming. Left, model with high viscosity ($\alpha = 10^{-2}$) and massive initial disk ($M_d(0) = 10^{-1} M_\odot$). The curves represent $t = 0, 2 \times 10^5, 4 \times 10^5, 4.7 \times 10^5, 4.8 \times 10^5, 4.9 \times 10^5, 5 \times 10^5, 5.1 \times 10^5, 5.2 \times 10^5, 5.3 \times 10^5 \text{ yr}$. The disk edge reaches the EUV gravitational radius at $t_{R_{gII}} \sim 4.9 \times 10^5 \text{ yr}$, when the disk mass is $\sim 10^{-6} M_\odot$. The disk mass corresponding to the last surface density distribution shown (at $t = 5.3 \times 10^5 \text{ yr}$) is $\sim 10^{-9} M_\odot$. Right, model with low viscosity ($\alpha = 10^{-3}$) and small initial disk ($M_d(0) = 10^{-2} M_\odot$). The curves represent $t = 0, 10^3, 10^4, 10^5, 2 \times 10^5, 3 \times 10^5, 4 \times 10^5, 5 \times 10^5, 6 \times 10^5, 7 \times 10^5, 8 \times 10^5, 9 \times 10^5, 10^6, 1.1 \times 10^6, 1.2 \times 10^6 \text{ yr}$. The disk edge reaches the EUV gravitational radius at $t_{R_{gII}} \sim 6 \times 10^5 \text{ yr}$, when the disk mass is $\sim 10^{-5} M_\odot$. The disk mass corresponding to the last surface density distribution shown (at $t = 1.2 \times 10^6 \text{ yr}$) is $\sim 10^{-9} M_\odot$.

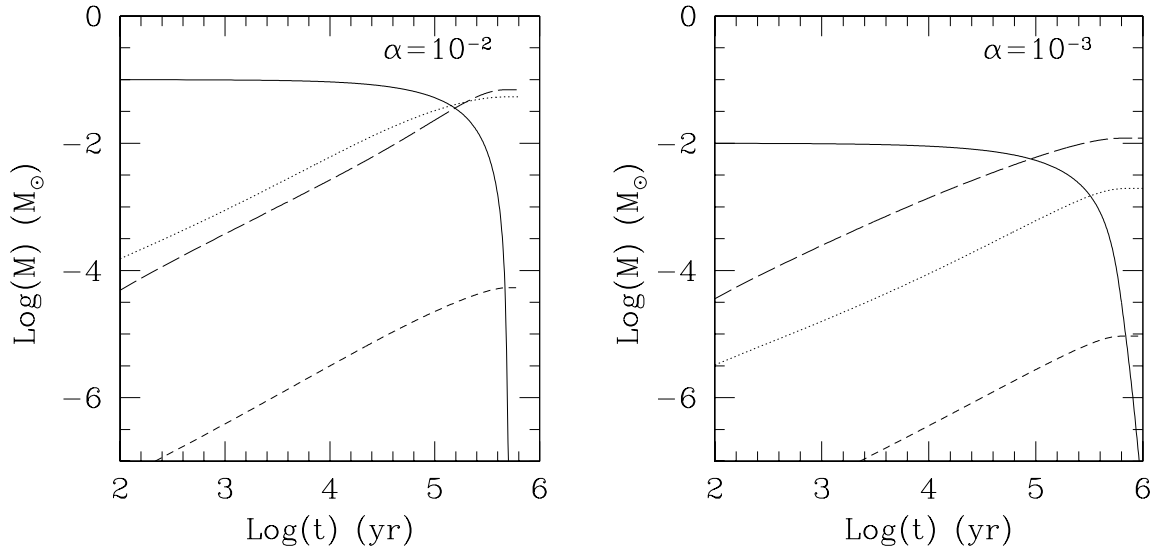


Fig. 6.— Disk mass (solid line), disk mass accreted toward the central star (dotted line), disk mass removed by photoevaporation from the central source (short-dashed line), and disk mass removed by EUV photoevaporation by external stars (long-dashed line) vs. disk lifetime for the two representative models.

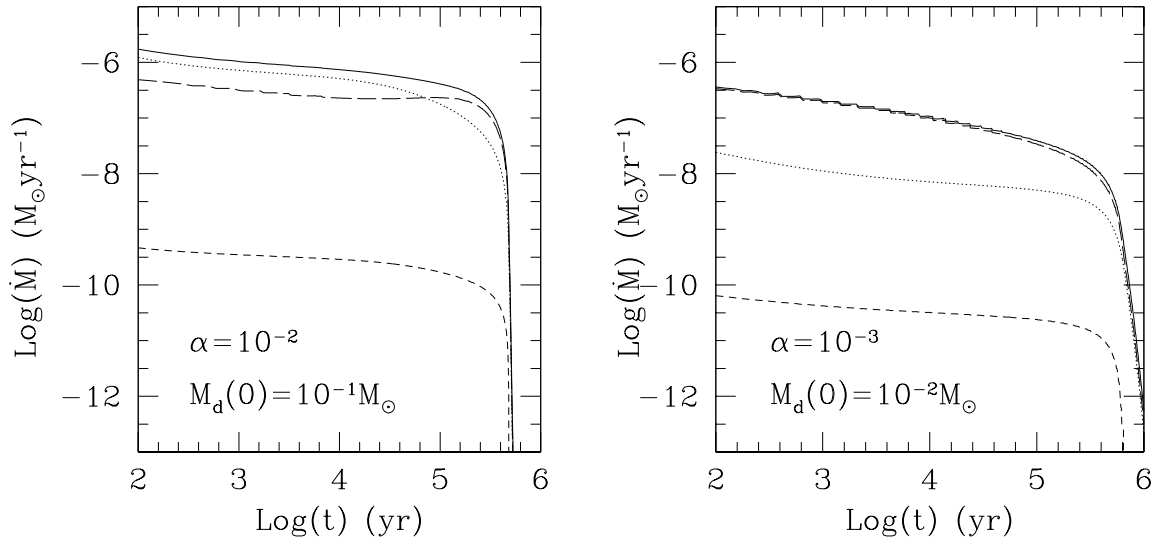


Fig. 7.— Total mass removal rate (solid line), mass removal rate due to accretion (dotted line), mass removal rate due to photoevaporation by the central source (short-dashed line), and disk mass removed by EUV photoevaporation by external stars (long-dashed line) as a function of disk lifetime for the two representative models. The disk is removed by viscous diffusion, photoevaporation from the central source, and EUV photoevaporation by external stars.

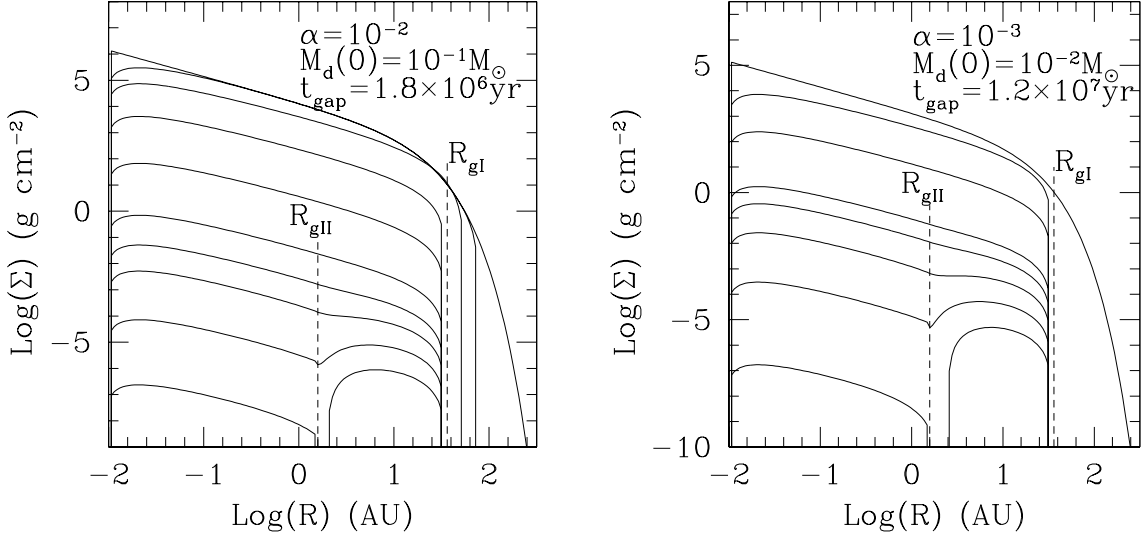


Fig. 8.— Snapshots of the surface density for two representative models with viscous diffusion, photoevaporation from the central source, and EUV photoevaporation by external stars. The dashed lines indicate the location of the EUV gravitational radius, r_{gII} , the FUV gravitational radius, r_{gI} . A gap structure forms at $t \sim t_{gap}$. Left, model with high viscosity ($\alpha = 10^{-2}$) and massive initial disk ($M_d(0) = 10^{-1} M_\odot$). The curves represent $t = 0, 10^3, 10^5, 5 \times 10^5, 10^6, 1.5 \times 10^6, 1.7 \times 10^6, 1.8 \times 10^6, 1.9 \times 10^6$, and 2×10^6 yr. The disk edge reaches the FUV gravitational radius, R_{gI} , at $t \sim 10^5$ yr, when the disk mass is $\sim 3 \times 10^{-2} M_\odot$. A gap structure forms at $t_{gap} \sim 1.8 \times 10^6$ yr, when the disk is almost completely removed ($M_d \sim 10^{-8} M_\odot$). The disk mass corresponding to the last surface density distribution shown (at $t = 2 \times 10^6$ yr) is $\sim 10^{-10} M_\odot$. Right, model with low viscosity ($\alpha = 10^{-3}$) and small initial disk ($M_d(0) = 10^{-2} M_\odot$). The curves represent $t = 0, 10^6, 5 \times 10^6, 10^7, 1.1 \times 10^7, 1.2 \times 10^7, 1.3 \times 10^7$, and 1.4×10^7 yr. The disk edge is reduced to the FUV gravitational radius, R_{gI} , at $t \sim 10^6$ yr, when the disk mass is $\sim 4 \times 10^{-3} M_\odot$. A gap structure starts forming at $t_{gap} \sim 1.2 \times 10^7$ yr, when the disk mass is reduced to $\sim 10^{-7} M_\odot$. The disk mass corresponding to the last surface density distribution shown (at $t = 1.4 \times 10^7$ yr) is $\sim 10^{-9} M_\odot$.

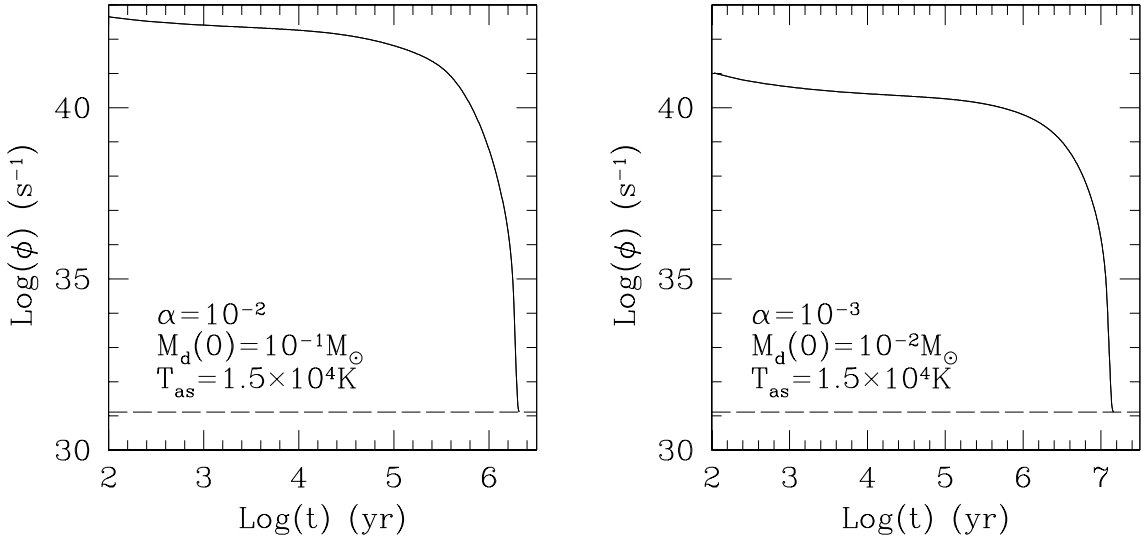


Fig. 9.— Ionizing flux from the central source for disk removal by viscous accretion, photoevaporation from the central source, and FUV photoevaporation by external stars as a function of disk lifetime. The ionizing flux decreases at late stages of the disk evolution with the accretion rate. The long-dashed line indicates the constant ionizing flux from the quiescent stellar photosphere ($\phi_{\star} = 1.29 \times 10^{31} \text{s}^{-1}$).

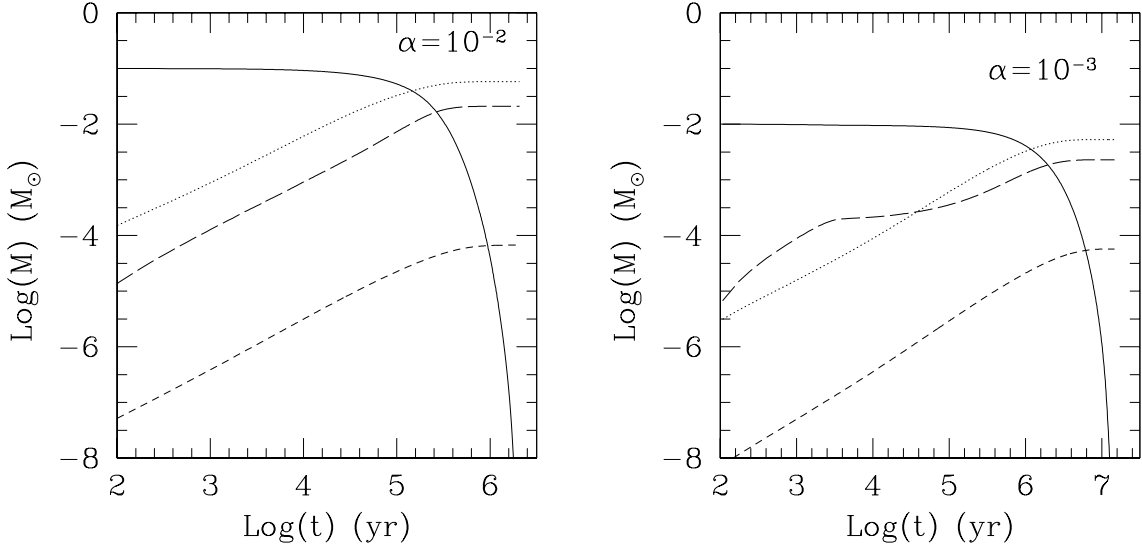


Fig. 10.— Disk mass (solid line), disk mass accreted toward the central star (dotted line), disk mass removed by photoevaporation from the central source (short-dashed line), and disk mass removed by FUV photoevaporation by external stars (long-dashed line) vs. disk lifetime for the two representative models.

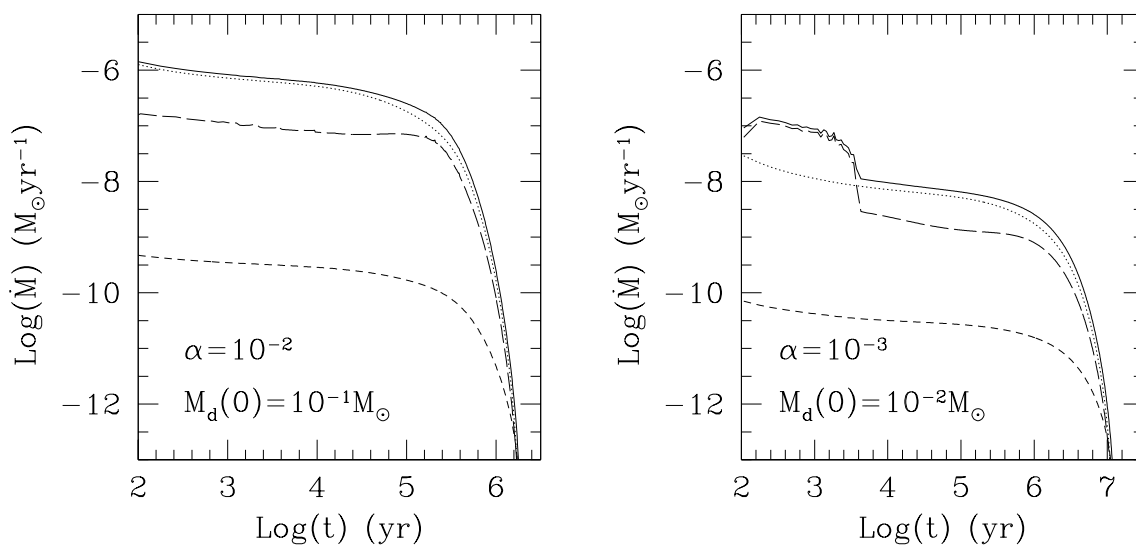


Fig. 11.— Total mass removal rate (solid line), mass removal rate due to accretion (dotted line), mass removal rate due to photoevaporation by the central source (short-dashed line), and mass removal rate by the external stars (long-dashed line) as a function of disk lifetime for the two representative models. The disk is removed by viscous diffusion, photoevaporation from the central source, and FUV photoevaporation by external stars.